DESIGNING A CERAMIC PARTICULATE COMPOSITE TO ENHANCE SELECTED MECHANICAL PROPERTIES OF Ti6Al4V

M. Seleso*[1], M. Maringa[2] & W. du Preez[3]

[1]Department of Mechanical and Mechatronics Engineering, Central University of Technology, Free State. masenate.a.thamae@gmail.com

[2] Department of Mechanical and Mechatronics Engineering, Central University of Technology, Free State, mmaringa@cut.ac.za

[3] Centre for Rapid Prototyping and Manufacturing, Faculty of Engineering, Built Environment and Information Technology, Central University of Technology, Free State, wdupreez@cut.ac.za

ABSTRACT

Particle reinforced metals provide good specific strength, good specific stiffness, and isotropic properties. Ti6Al4V is mostly used in engineering applications due to its excellent combination of high specific strength, good fatigue properties and outstanding corrosion resistance. A limitation of titanium alloys such as Ti6Al4V is their poor abrasion resistance. This limitation of Ti6Al4V and other properties of this titanium alloy may be improved to extend its application in industries such as power generation, aviation, automotive and oil. This review examines the influence of ceramic particles as reinforcement on the mechanical properties of a Ti6Al4V matrix. The paper further examines the interface, failure mechanisms and thermal mismatch of the coefficient of expansion of ceramic/Ti6Al4V composites.

*Corresponding author

1. INTRODUCTION

Composite materials are defined as a combination of two or more materials that results in better properties than those of the individual components alone. Composites are comprised of two phases which are the reinforcement and matrix phases [1]. Matrices are usually tough and ductile, while reinforcing materials are strong, have high values of stiffness and low density [2].The properties of composites are mainly determined by the properties of the matrix and reinforcement and the interface formed between the two, with the interface playing an important role in the performance of composites [2]. Additive Manufacturing (AM) is a manufacturing technique capable of producing components with complex geometries while ensuring minimal wastage of raw material, compared to conventional subtractive manufacturing techniques, such as turning and milling. This study is a precursor to building of powder based SiC/Ti6Al4V composites using the Direct Metal Laser Sintering (DMLS) additive manufacturing process. Direct Metal Laser Sintering involves the selective melting and fusing of powder particles as a laser beam passes over a powder bed to form a part according to a stipulated geometry, in a layer upon layer process [3].

Ti6Al4V is commonly referred to as surgical titanium or medical titanium grade because it is able to resist corrosion from body fluids and hence is a metal of choice within the medical industry [4]. Ti6Al4V is a preferred alloy in the aerospace sector for the manufacture of airframes, landing gear and engine parts as it has excellent strength-to-weight ratio compared to steel and aluminium. It is stronger than steel but 45% lighter. The high specific strength of Ti6Al4V allows for the manufacture of light weight components and therefore provides a reduction of fuel consumption [5]. Ceramics are good for reinforcing Ti6Al4V as they have complementary properties of high melting temperatures, high specific stiffness, high specific strength, high hardness, high abrasion resistance and high fracture toughness.

The major failure mechanisms of particle reinforced metal matrix composites that depend on the behaviour of matrix and reinforcement include particle fracture, interface decohesion and matrix yielding. The mechanical properties of particulate reinforced metal matrix composites and their resistance to failure are strongly affected by methods of fabrication, interfacial bond strength, volume fraction, shape and size of particles, particle size distribution and properties of the constituents [6]. Interfacial decohesion is usually observed in composites with matrices of relatively low strength compared to that of the reinforcement particles, while particle fracture usually occurs for matrices with medium to high strength relative to the reinforcing phase. While not addressing incidences of matrix failure and strain related failure of the composite constituents, such failure is a departure from the predictions of theoretical modelling that assume perfect adhesion between the composite constituents till failure and has relevance in this work due to the different values of strength of SiC particles used in modelling here.

Interfacial fracture is initiated by the nucleation of a crack at the interface as the stress at the interface exceeds the interfacial bond strength, normally at the point where the stresses are maximum [7]. Damage increases as the crack propagates along the particle/matrix interface and the magnitude of load transferred from the matrix to the respective particle is reduced. For effective reinforcement, the particles should be small and evenly distributed throughout the matrix. The particulate phase is normally harder and stiffer than the matrix, and the reinforcing particles tend to restrain movement of the matrix phase near each particle. The matrix transfers some of the applied load to the particles and, therefore, the degree of reinforcement or improvement of mechanical behaviour depends on strong bonding at the matrix/particle interface [6].

Yun Fu et al. [8], studied the effects of particle size, particle/matrix interface adhesion and particle loading on the mechanical properties of particulate composites and found that for poorly bonded particles, cracks are attracted to the equator of particles and subsequently move round the particles. For well bonded particles, cracks are attracted to the poles of particles, and then propagate through the matrix above or below the respective particles [8].This and the preceding discussion would imply failure in particulate composites emanating from interfacial cracks for weakly bonded particles, and from cracking of particles during

deformation for strongly bonded particles, which in both cases then transits into the matrix. In addition to size effects of particles, irregularly shaped particles experience weakening due to stress concentrations, while for rounded particles the stress concentration is much less severe than for the irregularly shaped particles with their sharp corners. Therefore, large size particles and ones with elongated shapes are more prone to failure than small hemispherical ones [9]. Ebrahim et al. [10] studied the interfacial strength between the matrix and the reinforcing particles and also the effective surface of debonding particles and found that the debonding mechanism had a negligible effect on the toughness of composites. However, they found that the debonding mechanism had a considerable effect on the tensile strength of particulate reinforced composites [10]. This is symptomatic of the opposing effects of reduced ductility (increased brittleness) and increasing strength, respectively. These opposing trends will affect design with composite materials depending on the requirements of strength and ductility for the final product.

Rahman et al. [21] studied the mechanical properties and wear characteristics of silicon carbide (SiC) reinforced aluminium metal matrix composites and found that at 20vol% of SiC, maximum wear resistance, maximum tensile strength and hardness were achieved. Ghafar et al. [11] applied the rule of mixture (RoM) equations and the Halpin-Tsai semi-empirical equations to predict the modulus of particulate composites. They found that values of fracture stress calculated according to the Halpin-Tsai semi-empirical equations showed very good correlation with the experimentally determined values. At low volume fractions (up to 35%) the values of elastic modulus calculated using the Halpin-Tsai semi-empirical equations also showed good agreement with data obtained experimentally. However, as the volume fraction increased above this value, the calculated and experimental values diverged from each other considerably [11].

It is important to determine what the cut-off is and the rate of divergence of theoretical and experimental values above this cut-off for SiC/Ti6Al4V composite that is the focus of study here, as a way of determining whether the given cut-off is universal or specific to a specific composite. Dash et al. [11] reviewed the behaviour of aluminium matrix composites under thermal stresses. They found that under uniform changes of temperature, such as during cooling from fabrication temperatures, large thermal residual stresses were induced at the interfaces of the composite constituents due to thermal mismatch between the constituents. This is important in laser powder bed fusion (LPBF) of composites where high prevailing rates of cooling are likely to initiate cracks in the matrix and at the interfaces, which then act as sites around which eventual failure of composites occurs.

The purpose of this design is to develop a SiC/Ti6Al4V composite with increased hardness, strength and stiffness relative to those of Ti6Al4V as well as decreased coefficient of thermal expansion that is close to that of carbon fibre epoxy reinforced composites. Using several theories for predicting the properties of composites, this paper demonstrates the flexibility of composites in design, in this case SiC/Ti6Al4V composites, in producing materials to satisfy various needs as a function of the volume fraction of reinforcing fillers.

2. MATERIALS AND METHODS

The constituent components used in the present work are SiC and Ti6Al4V powders, with the mechanical properties shown in Table 1. The higher values of specific strength and stiffness, as well as higher values of hardness of SiC than Ti6Al4V imply that the combination of the two materials will create a composite with these improved properties over those of the Ti6Al4V matrix alone, while providing light weighting.

Table 1: Mechanical properties of SiC and Ti6Al4V powders [12, 13, 14]

	SiC	Ti6Al4V
Mechanical properties		
Tensile strength (MPa)	240- 1625	950
Specific tensile strength (kNm/kg)	75-490	211
Young's modulus (GPa)	410	110
Specific Stiffness (MNm/kg)	132	24
Knoop Hardness (MPa)	2800	363
Bulk modulus (GPa)	176	125
Shear Modulus (GPa)	45	44
Physical properties		
Coefficient of thermal expansion (10^{-6}/K)	4.2	8.6

The size and shape of particles affect the mechanical properties of particulate composites such as stiffness and strength. The modulus of a composite is insensitive to particle size for particle sizes above 20 - 30 nm up to the micro scale (1-5 μm), below which there is a significant increase of elastic modulus of composites [8]. The strength of reinforced composites increases continuously with increasing particles size. The interfacial bond strength of filler particles has no effect on the magnitude of elastic modulus of particulate composites due to the fact that the levels of loading are typically too low to cause expansion large enough to initiate interfacial separation. Moreover, the surfaces of nano particles are too small to facilitate stress transfer to the full strength of the reinforcing fillers [7]. However, the interfacial bond strength does support a continuous increase in the strength of particulate composites with increasing size of the reinforcing particles due to stress transfer through the interface [7]. Increasing the volume fraction of nano filler particles was noted to lead to an increase of stiffness and a decrease of strength [7]. The foregoing review shows that the size of reinforcing particles affects various mechanical properties of composites differently [15]. Particles with sharp corners lower the strength of composites due to effects of stress concentration, while spherical particles give rise to composites with higher values of Young's modulus. Table 2 gives a summary of the shape and size of particles used in the present work. The foregoing demands that morphological studies of particulate composites be carried out for constituent powders prior to and after mixing, and further, after build of the final products.

Table 2: The shape and size of SiC and Ti6Al4V particles used in the present work

Morphology of particles	SiC	Ti6AL4V
Shape	Spherical	Spherical
Size	<45 μm	20-45 μm

3. ANALYTICAL MODELLING

There are a number of analytical models used to predict the elastic behaviour of composite materials, including the Rule of Mixtures (RoM), Inverse Rule of Mixtures (IRoM), equations of Guth and, separately, Smallwood, Mooney Equation, Halpin-Tsai semi-empirical equations, Hashin and Strickman bounds, Kerner equations and the equations of McGee and McCullough

[9]. The Hashin and Strickman equations are widely used to predict the properties of particulate composites and fall between the upper and lower bounds [16]. Kerner equations are some of the most elaborate equations for a composite material consisting of spherical particles in a matrix. The assumption is made in these equations of perfect adhesion of the matrix and filler (particles). The Kerner equations are useful for composites reinforced with randomly dispersed spherical particles in a polymer and metal matrix [9]. For the reasons detailed in the next session, the Halpin-Tsai equations, the Rule of Mixtures and Inverse Rule of Mixtures equations are preferred for use here.

3.1 The Rule of Mixtures

The RoM, also known as the Voigt or iso-strain rule and the IRoM also known as the Reuss or iso-stress rule define the upper and lower bounds of the properties of composite materials, respectively. The assumptions are made in the methods that the constituent components of the composite are perfectly bonded together and that they deform together [2]. The upper and lower bounds are represented by the Voigt and Reuss rules shown as equations (1) and (2), and (3), respectively [17]:

$$E_c = E_m \upsilon_m + E_p \upsilon_p \tag{1}$$

$$\sigma_c = \sigma_m \upsilon_m + \sigma_p \upsilon_p \tag{2}$$

$$E_c = \frac{E_m E_p}{E_m \upsilon_p + E_p \upsilon_m} \tag{3}$$

In these equations, the symbols, E,υ, c, m, p σ_c denote elastic modulus, volume fraction, composite, matrix, particulate phases and strength of composites respectively [17].The Reuss and Voigt rules are also used to predict the coefficient of thermal expansion of composites. The Reuss Rule leads to the following expression of the coefficient of thermal expansion.

$$\alpha_c = \frac{V_m E_m \alpha_m + V_p E_p \alpha_p}{V_m E_m + V_p E_p} \tag{4}$$

Where the symbols α_c, $\alpha_{m,}$ α_p represent the thermal expansion coefficients of the composite, matrix and particles, respectively. The Voigt model, which assumes uniform strain in a composite after the uniform change of temperature, leads to an expression for effective Coefficient of Thermal Expansion (CTE) as follows;

$$\alpha_c = V_m \alpha_m + V_p \alpha_p \tag{5}$$

The RoM is not useful for making predictions in the transverse direction of reinforcing fibres and often overestimates the ultimate tensile strength of unidirectional fibre reinforced composites [18]. The RoM does not take into account the aspect ratios of reinforcing particles and is inexact in estimating the effective modulus of particulate metal matrix composites. However, it is more exact in the longitudinal direction of continuous fibre reinforcement with high aspect ratios. It is for this reason that the IRoM is used to predict the values of elastic modulus for composites in the transverse direction.

3.2 The Halpin-Tsai Semi Empirical Equations

The Halpin-Tsai semi-empirical model is the most widely used model to predict the elastic moduli of composites, though it suffers the drawback of being dependent on parameters that need to be determined experimentally. The Halpin-Tsai semi-empirical model predicts the transverse Young's modulus and the shear modulus of composite materials [17, 19]. For composites with aligned fibres, the Halpin-Tsai semi-empirical model defines the transverse Young's modulus as follows;

$$E = \frac{E_m(1+\eta\xi v_f)}{(1-\eta v_f)} \tag{6}$$

$$\eta = \frac{{E_f}/{E_m} - 1}{{E_f}/{E_m} + \xi} \tag{7}$$

In this equation, the parameters E_f and E_m denote the elastic modulus of fibre and matrix respectively, V_f the volume fraction of fibre, η a stress partitioning factor and ξ a shape factor which measures the reinforcing efficiency and depends upon the geometry and distribution or packing arrangement of the reinforcing fibres and the direction of loading [17, 19]. When the value of ξ becomes very small ($\xi \to 0$) the Halpin-Tsai semi-empirical model reduces to the IRoM or Reuss rule. For composites with large values of ξ($\xi \to \infty$), the Halpin-Tsai semi-empirical model reduces to the RoM or Voigt rule. For composites reinforced with randomly oriented fibres, the Halpin-Tsai semi-empirical equations are more elaborate and take the form;

$$E_c = E_m\left[\frac{3}{8}\left(\frac{1+\xi\eta_l V_f}{1+\eta_l V_f}\right) + \frac{5}{8}\left(\frac{1+2\eta_T V_f}{1-\eta_T V_f}\right)\right] \tag{8}$$

In Equation 8, the symbols (η_l andη_T) stand for;

$$\eta_l = \frac{{E_f}/{E_m} - 1}{{E_f}/{E_m} + \frac{2l}{d}} \tag{9}$$

$$\eta_T = \frac{{E_f}/{E_m} - 1}{{E_f}/{E_m} + 2} \tag{10}$$

The Halpin-Tsai semi-empirical equations are good for predicting properties at low volume fractions of the reinforcing phase but underestimate the properties at high volume fractions. The Halpin-Tsai equations allow sensible interpolations to be made between the upper and lower bounds of composite properties. They offer the advantage of being simple and easy to use in design and give good predictions, though they suffer the setback of being dependent on parameters that need to be determined experimentally [19]. The Halpin-Tsai equations are also useful in determining the properties of composites that contain discontinuous fibres oriented in the loading direction. The Halpin-Tsai equations are seen from this review to be flexible and adaptable to model any type of composite, thus their preference here over other models.

3.3 Hashin and Strickman Model

The Hashin and Strickman equations are widely used to predict the properties of particulate composites and fall between the above mentioned lower and upper bounds [16]. They are described by the following equations;

The lower bound equation [16]

$$E_c = \frac{9\left[K_p + \frac{V_m}{\frac{1}{K_m - K_p} + \frac{3V_p}{3K_{p+4G_p}}}\right]\left[G_p + \frac{V_m}{\frac{1}{G_m - G_p} + \frac{6V_p(K_p+2G_p)}{5G_m(3k_m+4G_m)}}\right]}{3\left[K_p + \frac{V_m}{\frac{1}{K_m - K_p} + \frac{3V_p}{3K_{p+4G_p}}}\right] + \left[G_p + \frac{V_m}{\frac{1}{G_m - G_p} + \frac{6V_p(K_p+2G_p)}{5G_p(3k_p+4G_p)}}\right]} \quad (11)$$

In Equation 8, the symbols K and G represent the bulk and shear moduli, and the subscripts m and p refer to matrix and particle, respectively. The Poisson's ratio of composites in this model are given by the expression;

$$v_c = \frac{3K_c - 2G_c}{2(G_c + 3K_c)} \quad (12)$$

The upper bound Equation [16]

$$E_c = \frac{9\left[K_m + \frac{V_p}{\frac{1}{K_p - K_m} + \frac{3V_m}{3K_{m+4G_m}}}\right]\left[G_m + \frac{V_p}{\frac{1}{G_p - G_m} + \frac{6V_m(K_m+2G_m)}{5G_m(3k_m+4G_m)}}\right]}{3\left[K_m + \frac{V_p}{\frac{1}{K_p - K_m} + \frac{3V_m}{3K_{m+4G_m}}}\right] + \left[G_m + \frac{V_m}{\frac{1}{G_p - G_m} + \frac{6V_m(K_m+2G_m)}{5G_m(3k_m+4G_m)}}\right]} \quad (13)$$

The Hashin and Strickman equations are also used to predict the coefficient of thermal expansion of composites since the mixture rules do not give accurate results. The Hashin and Strickman expression for the coefficient of thermal expansion is as follows:

$$\alpha_c = \alpha_m + \frac{\alpha_p - \alpha_m}{1/E_p - 1/E_m}\left(1/E_c - 1/E_m\right) \quad (14)$$

4. MODELLING THE PROPERTIES OF SIC/TI6AL4V PARTICULATE COMPOSITES

The properties of SiC and Ti6Al4V given in Table 1 are used in Equations 1 and 2 to predict the values of strength and stiffness of composites of the materials at different volume fractions of the reinforcing SiC particles. Figure 1 shows the strength of composites of SiC/Ti6Al4V with varying volume fractions of SiC particles from zero to 100vol%, based on the Voigt rule for both high and low values of strength of SiC particles.

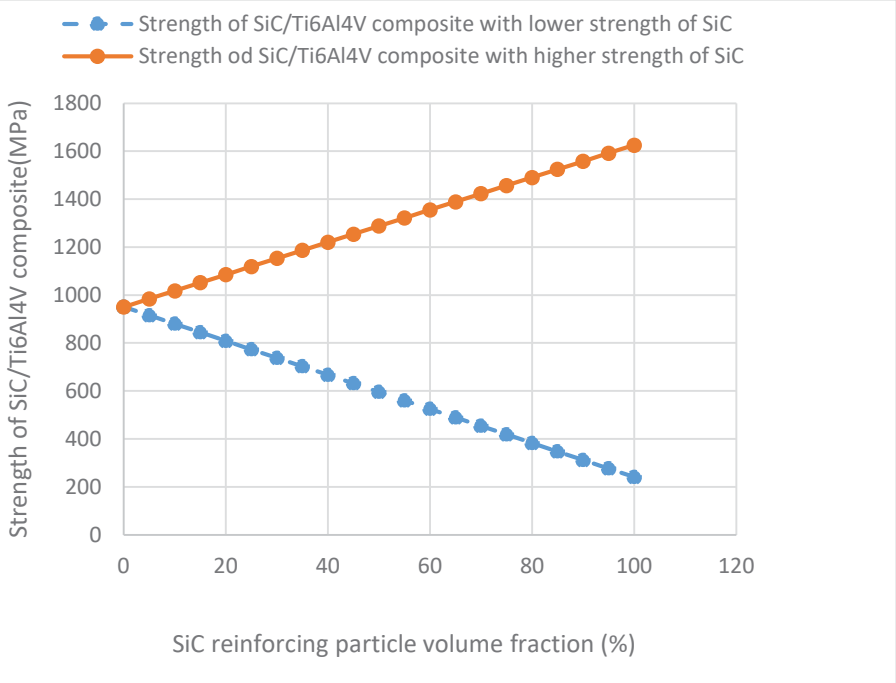

Figure 1: Curves of the strength of SiC/Ti6Al4V composites versus volume fraction of SiC particles based on the Voigt Rule for high and low strength of SiC particles

The curve of the composite with SiC particles of higher strength (continuous curve) is seen to increase with increasing volume fraction of the particles while that with the SiC particles of lower strength (hatched curve) is seen to decrease with increasing volume fraction of the particles. At 20% volume fraction, the hatched curve shows a composite strength of 808 MPa, which is lower than that of Ti6Al4V (950 MPa) and higher than that of SiC (240 MPa); a 15% drop in the strength of Ti6Al4V. At the same volume fraction of SiC filler, the continuous curve shows a composite strength of 1085 MPa, which is higher than that of Ti6Al4V and lower than that of the higher SiC value of 1625 MPa; a 14% enhancement of the strength of Ti6Al4V. The particulate filler volume fraction of 20vol% is used here based on the work of Ramah et al. [21] for SiC/Al composites, which showed that filler volume fractions above this volume fraction in MMCs lead to increase in the hardness of the particles, thus encouraging initiation of cracks at the interface and consequent failure of the composites. Figure 2 shows the elastic modulus of SiC/Ti6Al4V composite with varying volume fraction of SiC particles.

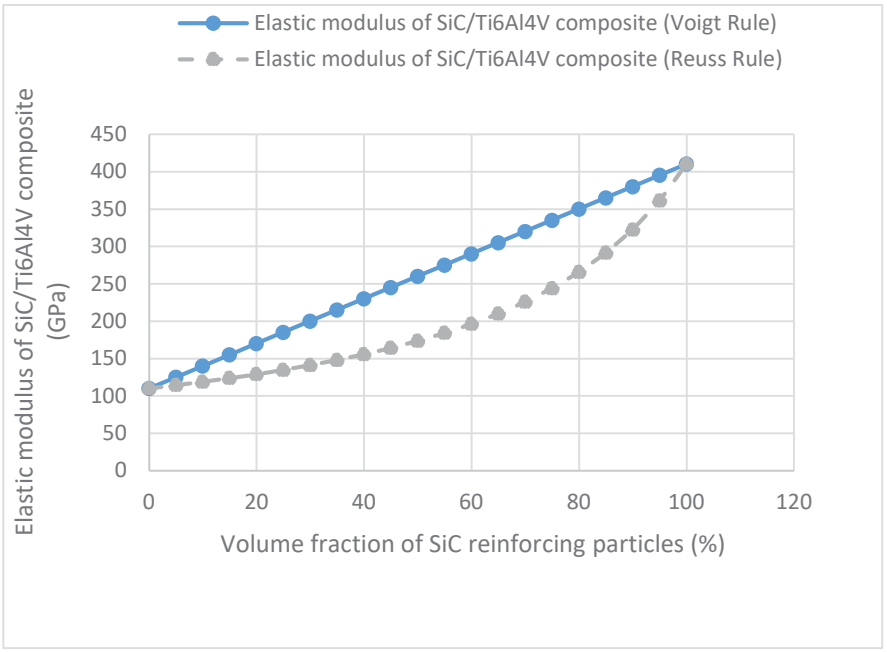

Figure 2: Elastic modulus of SiC/Ti6Al4V composite with varying volume fraction of SiC particles

It is seen from the graph that the rate of increase of stiffness of a composite increases with increasing volume fraction of the reinforcing particles. At a volume fraction of the reinforcing SiC particles of 20%, the curve for the IRoM gives a value of the elastic modulus of the SiC/Ti6Al4V composite of 130 GPa which is higher than that of Ti6Al4V (110 GPa) and lower than that of the SiC particles (410 GPa). This is an 18% increase in modulus over that of Ti6Al4V. At the same volume fraction, the Voigt curve gives a value of 170 GPa; a 55% increase in modulus over that of Ti6Al4V. At a volume fraction of the reinforcing SiC particles of 40%, the Reuss curve gives a value of 156 GPa while the Voigt rule gives a value of 230 GPa; increases of 42% and 109 % over that of Ti6Al4V, respectively. The higher and lower values predicted by the Voigt and Reuss rules, respectively, are not surprising as the first rule defines the upper bound while the Reuss rule defines the lower bound for composites. The reinforcing volume fractions of 20% and 40% are selected for analysis here based on the separate works of Ramah et al. [21] and Yilmaz et al. [20] that showed the former and the latter to be limiting volume fractions at which cracks at the interfaces were initiated and where maximum stiffness of particulate composites occurred, respectively.

Equations 8, 2 and 1 are used to plot values of the elastic modulus of SiC/Ti6Al4V composites with varying volume fractions of SiC particles, with the results shown in Figure 3. A shape parameter ξ=2 was used as recommended by Halpin_Tsai for predictions of elastic modulus [1] and the ratio (l/D) for the stress partitioning factor (η_l) set to unity for idealised shperical particles. Equation 6 was used here instead of Equation 5 as it models randomly oriented short fibres, which better approximates particle fillers when their aspect ratio (l/D) is set to unity.

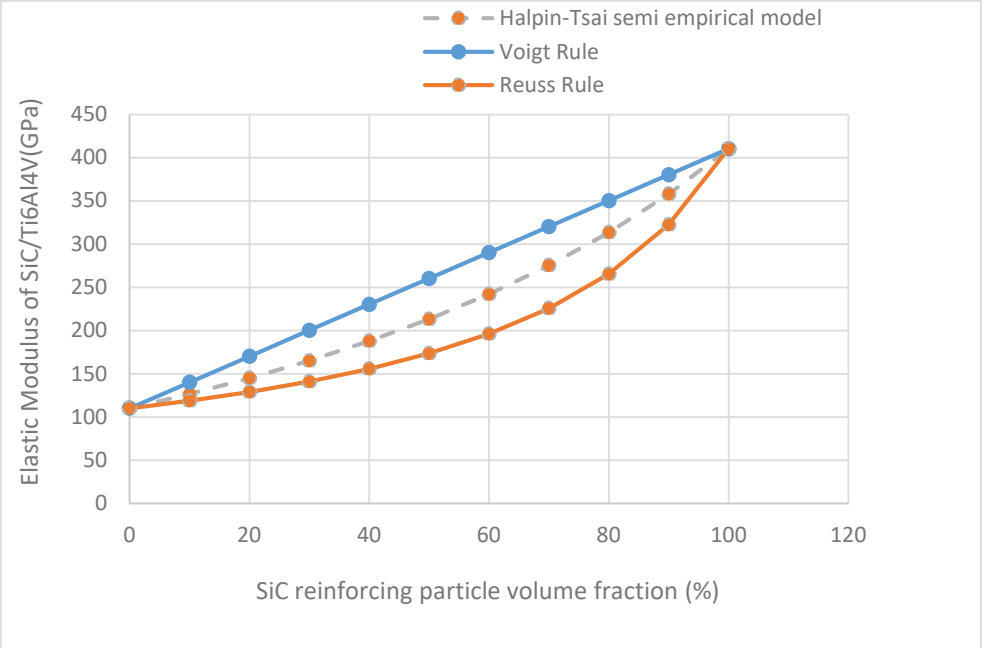

Figure 3: The curves of Reuss, Voight and Halpin-Tsai Semi-Empirical Equations

All the three curves in Figure 3 show effective reinforcement at all volume fractions of the SiC reinforcing particles. At 20% volume fraction, the Voigt, Halpin-Tsai semi-empirical equations, and Reuss curves show values of elastic modulus for SiC/Ti6Al4V composites of 170 GPa, 145 GPa and 129 GPa, respectively. This translates to increases of 55%, 31%, and 17% respectively. At a volume fraction of 40%, the Voigt, Halpin-Tsai semi-empirical equations and Reuss curves show values of elastic modulus for SiC/Ti6Al4V composites of 230 GPa, 188 GPa, and 155 GP, respectively, which work out to improvements of elastic modulus over that of Ti6Al4V of 110%, 70%, 41% in the same order.

The Halpin-Tsai semi-empirical curve can be reduced to the lower or upper bound depending on the magnitude of the shape parameter (ξ). When the value of ξ becomes very small ($\xi \rightarrow 0$) the Halpin-Tsai semi-empirical model tends to the IRoM or Reuss rule. For large values of ($\xi \rightarrow \infty$), the Halpin-Tsai semi-empirical model tends to the RoM or Voigt rule. Figure 4 shows plots of the Halpin-Tsai semi-empirical equation for randomly oriented short fibres with the shape parameter ξ set to 0.05, 0.5, 1, 2, 5, 10, and 5000.

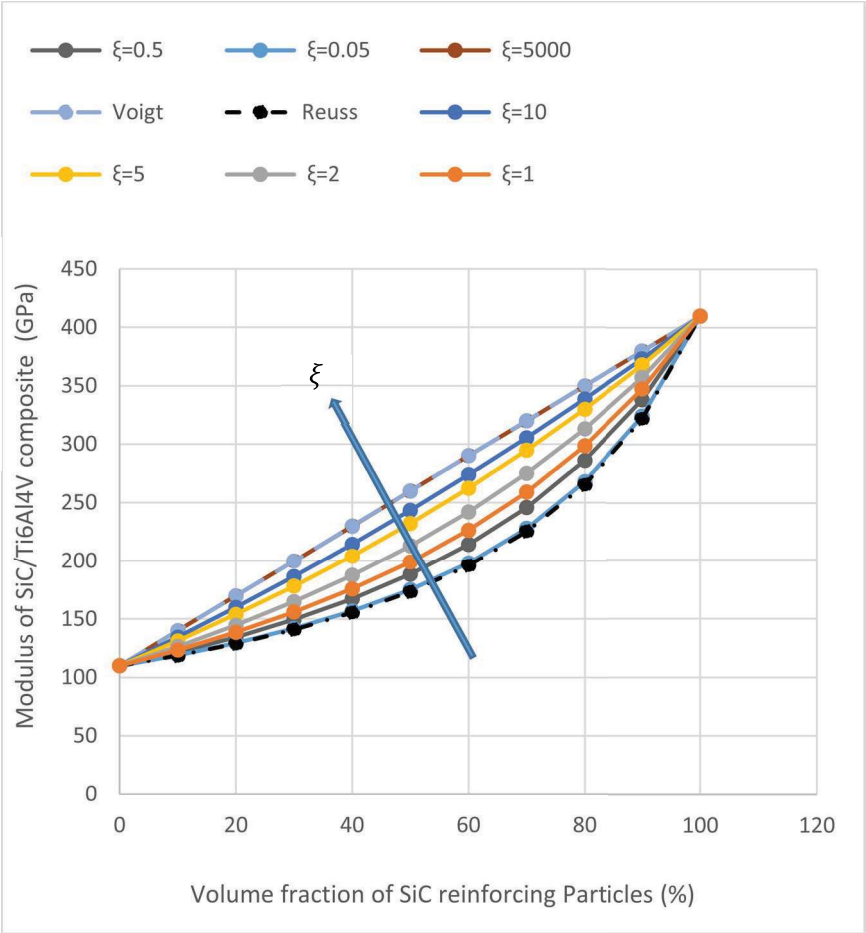

Figure 4: Plots of Halpin-Tsai Semi-Empirical Curves with Different Shape Parameters

It is observed from the graph that as the value of the shape parameter increases, the curves of elastic modulus tend to the Voigt curve. The curve with the largest value of shape parameter of 5000 plotted in this figure is seen to coincide with the Voigt curve. It is further observed from the graph that as the value of the shape parameter decreases towards zero, the curves approach the Reuss curve. The curve with the smallest value of 0.05 is seen in the figure to coincide with the Reuss curve. The power of the Halpin-Tsai semi-empirical equations is seen in the variation of the curves with changing values of the shape factor, as this enables the curves to be fitted to composites with widely varying values of elastic modulus.

The values of the coefficient of thermal expansion of SiC and Ti6Al4V in Table 1 are used in Equations 4, 5 and 14 to plot curves of the CTE for SiC/Ti6Al4V composites. Figure 5 shows plots of Reuss, Voigt and Hashin and Strickman (HS) models for predicting CTEs of SiC/Ti6Al4V composites with varying volume fractions of SiC particles.

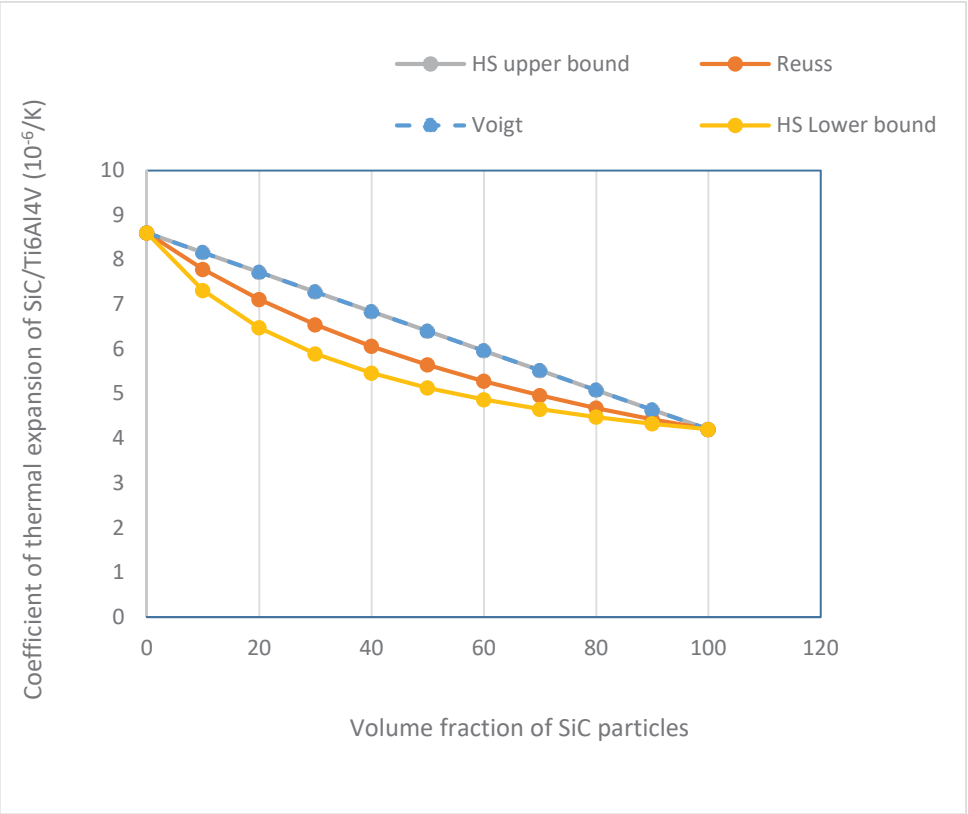

Figure 5: Plots of Voigt, Reuss and Hashin and Strickman models for predicting CTE of SiC/Ti6Al4V composites with varying volume fractions of SiC particles

The coefficient of thermal expansion is seen to decrease with increasing volume fraction of SiC particles. At a volume fraction of 20%, the CTE predicted by the HS lower bound is 6.5 x 10^{-6}/K, the Reuss rule 7.71×10^{-6}/K and HS upper bound and Voigt rule the same value of 7.72 x 10^{-6}/K. The CTE in these models is lower than that of Ti6Al4V (8.6 x 10^{-6}/K) and higher than that of carbon fibre/epoxy reinforced composites sheets of (2.1× 10^{-6}/℃) and carbon fibre tubes of 0.1× 10^{-6}/℃ . At a volume fraction of 40%, HS lower bound predicts a CTE of 5.5 x 10^{-6}/K, the Reuss rule 6.06× $10^{-6}/K$ and the HS upper bound and Voigt rule 6.8 x 10^{-6}/K. At this volume fraction, the predicted values of CTE by these three models are all lower than the values predicted at a volume fraction of 20%. Clearly, by closely matching the CTEs of SiC/Ti6Al4V composites to those of carbon fibre epoxy resin composites, the effects of differential expansion and contraction at their joints during thermal cycling can be reduced.

Reuss and Voigt models can also be used to explore the hardness (*H*) of SiC/Ti6Al4V thus.

$$H_c = H_m V_m + H_p V_p \tag{11}$$

$$H_c = \frac{H_m H_p}{H_m \upsilon_p + H_p \upsilon_m} \tag{12}$$

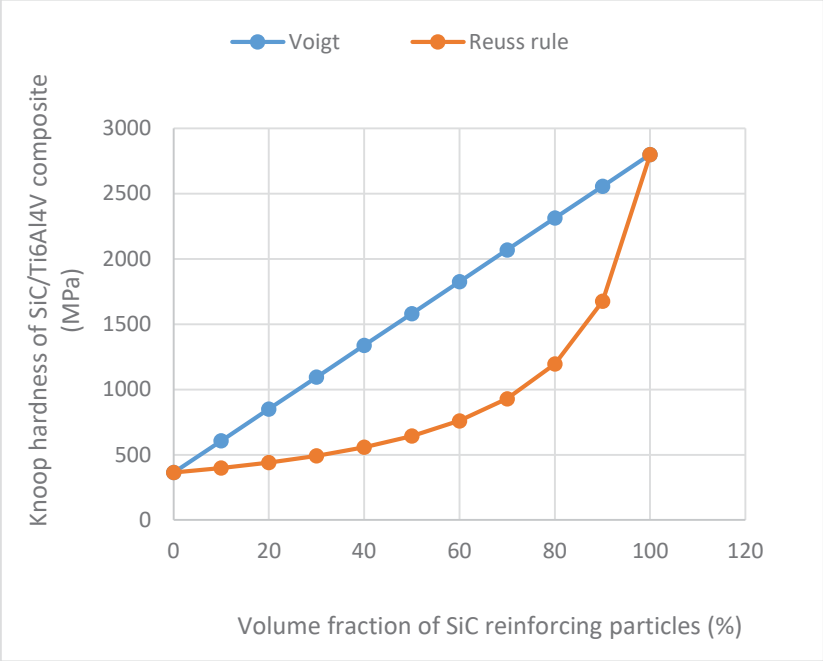

Figure 6: Theoretical values of the hardness of the SiC/Ti6Al4V composite

In Figure 6, the Voigt and Reuss rules predict values of hardness for the SiC/Ti6Al4V composite at a volume fraction of 20% of 850 MPa and 440 MPa, respectively. At a volume fraction of 40%, the Voigt and Reuss models predict values of hardness of 1338 MPa and 557 MPa, respectively. Both curves show that the hardness of SiC/Ti6Al4V increases with the increasing volume fraction of SiC reinforcing particles.

Figure 7 shows values of the hardness of SiC/Al, determined experimentally in the work of Yilmaz et al. [20].

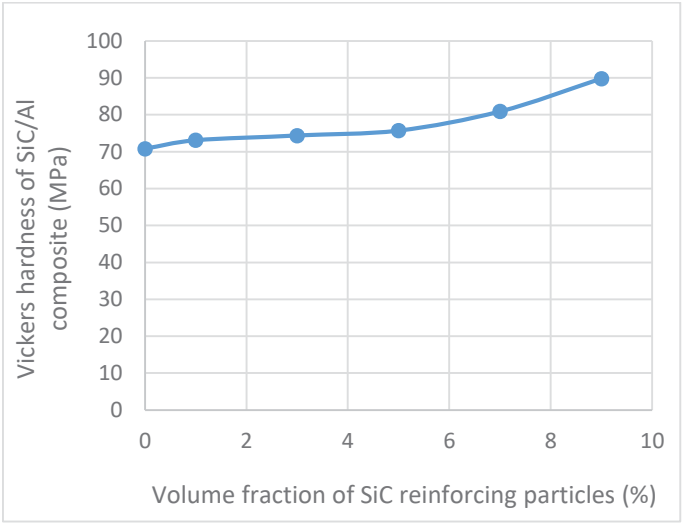

Figure 7: Experimental results of hardness of SiC/Al composite

Aluminium is considered a ductile metal as so is titanium. The hardness of the SiC/Al composite is seen to increase from 70.3 MPa at a volume fraction of the reinforcing SiC filler of 0% to a value of 89.8 MPa at a filler volume fraction of 10%. The curve in the figure shows an initial very low rate of increase that picks up with increasing volume fraction, which is consistent with the curve for the Reuss rule in Figure 6. This would imply the lower bound Reuss model gives better prediction than the upper bound Voigt rule

5. CONCLUSIONS

The study confirmed that it is indeed possible to design SiC/Ti6Al4V particulate composites with improved stiffness, hardness, strength, and coefficient of thermal expansion as detailed below. This study further demonstrated the flexibility of designing with composites materials that allows composites of different properties to be produced to meet required needs, as follows:

- Increasing the volume fraction of SiC particles above 40%vol increases hardness and strength but encourages the initiation of cracks at SiC/matrix interfaces leading to composite failure.
- At a volume fraction of reinforcing SiC filler of 20%, the Voigt rule predicted a 14% increase in strength, a 55% increase in stiffness, and a 53% increase in hardness. At the same volume fraction, the Reuss rule predicted an 18% increase in stiffness and 62% increase in hardness.
- At 40% volume fraction of SiC particles, the Voigt rule predicted a 28% increase in strength, 109% increase in stiffness, and 37% increase in hardness. The Reuss rule showed an increase of 43% in stiffness and 57% in hardness. The Halpin-Tsai semi-empirical rules predicted a 71% increase in stiffness.
- SiC/Ti6Al4V composites are likely to fail through particle fracture failure mechanisms as this usually occurs for matrices with medium or higher strength compared to that of the reinforcing phase.
- The study has showed that it is possible to obtain values of CTE for SiC/Ti6Al4V composites that are lower than those of Ti6Al4V even at the lowest volume fraction of reinforcing filler, with lower bound values of 6.5×10^{-6}/K and 5.5×10^{-6}/K at 20% and 40% volume fraction of reinforcing filler, respectively.
- The preferred model for predicting the elastic modulus of SiC/Ti6Al4V is the Halpin-Tsai semi empirical model because it allows sensible interpolations between the upper and the lower bounds. For predicting the CTE of SiC/Ti6Al4V composites, Hashin and Strickman upper bound coincides with the Voigt rule while the Hashin and Strickman lower bound falls below the Reuss rule and is therefore a poor model to use. For hardness of composites, it has been shown that the fit of the two theoretical models is dependent on the range of volume fraction under consideration.

REFERENCES

[1] Harris, B.1999. *Engineering Composite Materials*, Institude of Materials, London.

[2] Campbell, F.C. 2010. *Introduction to Composite Materials*, ASM International.

[3] Donachie, J. 2018. *Properties and Applications of Titanium and its Alloys*, ASM International, United States.

[4] Veiga, C., Davim, J.P., and Louveiro, A. J.R. 2012. Properties and Applicactions of Titanium Alloys, *Revised Advanced Material*, 32, pp. 133-148.

[5] Sozhamannan, G.G., Balasivanandha, S.P., and Raskaramoorth, R. 2010, Failure analysis of particle reinforced metal matrix composites by microstructure based models, *Materials and Design*, 31, pp. 3785-3780.

[6] Liu,H.T., Sun, L.Z., Ju, J.W. 2004. An Interface Debonding Model for Particle-reinforce composites, *International Journal of Damage Mechanics*, 13(2), pp. 163-185.

[7] Yun Fu S.Y, Feng X. Lauke B and Wing Mai, 2008. Effects of particle size, particle/matrix interface adhesion and particle loading on mechanical properties of particulate–polymer composites, *Composites: Part B,* 39, pp. 933-961.
[8] Ahmed, S. 1990. A review of particulate reinforcement theories for polymer composites, *Journal of material Science,* 25, pp. 4933-4942.
[9] Ebrahim S.V, Niaki K.S S.V, 2005. Design of metal matrix composites with particulate reinforement produced by deeep cryogenic treatment, *Material Science and Engineering,* 87, pp. 1-6.
[10] Ghafar, M.A., Mazen, A.A., Mahallawy, N.A. 2006**.** Application of the rule of mixtures and Halpin-Tsai equations to Woven Fabric reinforced epoxy composites, *Journal of Engineeering Sciences,* 34, pp. 227-236.
[11] Dash, K., Suku, Maran,L., and Ray,B.L. 2014. The behaviour of aluminium matrix composites under thermal stresses, *Science and Engineering of Composite Materials,* 23(1). pp.1-7.
[12] Committee, A.I. 1990**.** *Properties and Selection of non-ferous alloys and special purpose materials,* ASM International.
[13] Veiga, C., Davim, J.P., and Louveiro, A.J.R.2012, Properties and Applicactions of Titanium Alloys, *Revised Advanced Material,* 32, pp. 133-148.
[14] Shivakumar, K.S., and Doddamani. 2015**.** Characterization of mechanical properties of SiC/Ti6Al4V metal matrix composite using finite element method, *American journal of Material Science,* 5, pp. 78-11.
[15] Maringa, M. 2018. Improving the predictive capacity of Newtonian fluid theories on the elastic moduli ratio(Ec/Em) of particulate composites, *Eleventh South African Conference on Computational and Mechanics*, Vanderbijilpark.
[16] Sharma, S.K., Chandra, A., Kumar, A., Sighn, S.K. 2018, Modeling of Elastic Properties of Particulate Composites, *International Journal of Applied Engineering Research,* 13, pp. 263-267.
[17] Ahmed, F.S. 1990. A Review of Particulate Reinforcement theories for Polymer Composites, *Journal of Material Science,* 25, pp. 4933-4942.
[18] Zironng, H.L.X. 2018. Modified rule of mixtures and Halpin-Tsai model for predictionof tensile strength of micron sized reinforced composites and youngs modulus of multiscale reinforced composites for direct fabrication, *Advances in Mechanical Engineering,* 10(07), pp. 1-10.
[19] Osoka, E.C., Onukwuli, O.D. 2018. A modified Halpin-Tsai model to estimate the modulus of natural fibre reinforced composites, *International Journal of Engineering Science Invention,* 7(05), pp. 63-70.
[20] Yilmaz, O.,Turan, B.C. Gurbuz, M. 2019. Production and Caharecterisation of SiC reinforced alluminim alloy matrix composites from waste beverages cans, *Journal of Metals and Minerals,* 29(04), pp. 28-33**.**
[21] Rahman, M.H., Mamun, H.M.R. 2014. Characterisation of Silicon carbide reinforced Aluminum composites, *Procedia Engineering,* 90, pp. 103-109.